nature portfolio

Corresponding author(s): Huisken, Jan

Last updated by author(s): Sep 10, 2025

Reporting Summary

Nature Portfolio wishes to improve the reproducibility of the work that we publish. This form provides structure for consistency and transparency in reporting. For further information on Nature Portfolio policies, see our Editorial Policies and the Editorial Policy Checklist.

Statistics

For all statistical analyses, confirm that the following items are present in the figure legend, table legend, main text, or Methods section.

n/a	Confirmed	
☐	☒	The exact sample size (*n*) for each experimental group/condition, given as a discrete number and unit of measurement
☒	☐	A statement on whether measurements were taken from distinct samples or whether the same sample was measured repeatedly
☒	☐	The statistical test(s) used AND whether they are one- or two-sided *Only common tests should be described solely by name; describe more complex techniques in the Methods section.*
☒	☐	A description of all covariates tested
☒	☐	A description of any assumptions or corrections, such as tests of normality and adjustment for multiple comparisons
☐	☒	A full description of the statistical parameters including central tendency (e.g. means) or other basic estimates (e.g. regression coefficient) AND variation (e.g. standard deviation) or associated estimates of uncertainty (e.g. confidence intervals)
☒	☐	For null hypothesis testing, the test statistic (e.g. *F*, *t*, *r*) with confidence intervals, effect sizes, degrees of freedom and *P* value noted *Give P values as exact values whenever suitable.*
☒	☐	For Bayesian analysis, information on the choice of priors and Markov chain Monte Carlo settings
☒	☐	For hierarchical and complex designs, identification of the appropriate level for tests and full reporting of outcomes
☒	☐	Estimates of effect sizes (e.g. Cohen's *d*, Pearson's *r*), indicating how they were calculated

Our web collection on statistics for biologists contains articles on many of the points above.

Software and code

Policy information about availability of computer code

Data collection	The custom codes developed in this study have been deposited in the public repository GitHub (https://github.com/aakhtemostafa/Voice-Coil-Waveform-Correction.git).
Data analysis	Data and image processing, and visualization were performed using open-source and commercial software. Initial image analysis was conducted using Fiji, while stitching and conversion to HDF5 were carried out with BigStitcher. 3D data visualization was performed using Imaris 9.7. Point spread funtion measurements were obtained using a custom Python script and Fiji, and the resolution calculations for the detection objective lens were performed in MATLAB. The scripts are available from the authors upon request.

For manuscripts utilizing custom algorithms or software that are central to the research but not yet described in published literature, software must be made available to editors and reviewers. We strongly encourage code deposition in a community repository (e.g. GitHub). See the Nature Portfolio guidelines for submitting code & software for further information.

Data

Policy information about availability of data

All manuscripts must include a data availability statement. This statement should provide the following information, where applicable:

- Accession codes, unique identifiers, or web links for publicly available datasets
- A description of any restrictions on data availability
- For clinical datasets or third party data, please ensure that the statement adheres to our policy

Due to the very large size of the imaging datasets generated in this study, a down-sampled version of the complete stitched dataset together with a representative high-resolution subset has been deposited in Zenodo (https://doi.org/10.5281/zenodo.17080861). The full original high-resolution dataset is available from the corresponding author upon reasonable request.
The CAD models of the custom parts are available at the following link: https://doi.org/10.5281/zenodo.17396943

Research involving human participants, their data, or biological material

Policy information about studies with human participants or human data. See also policy information about sex, gender (identity/presentation), and sexual orientation and race, ethnicity and racism.

Reporting on sex and gender	*Use the terms sex (biological attribute) and gender (shaped by social and cultural circumstances) carefully in order to avoid confusing both terms. Indicate if findings apply to only one sex or gender; describe whether sex and gender were considered in study design; whether sex and/or gender was determined based on self-reporting or assigned and methods used.* *Provide in the source data disaggregated sex and gender data, where this information has been collected, and if consent has been obtained for sharing of individual-level data; provide overall numbers in this Reporting Summary. Please state if this information has not been collected.* *Report sex- and gender-based analyses where performed, justify reasons for lack of sex- and gender-based analysis.*
Reporting on race, ethnicity, or other socially relevant groupings	*Please specify the socially constructed or socially relevant categorization variable(s) used in your manuscript and explain why they were used. Please note that such variables should not be used as proxies for other socially constructed/relevant variables (for example, race or ethnicity should not be used as a proxy for socioeconomic status).* *Provide clear definitions of the relevant terms used, how they were provided (by the participants/respondents, the researchers, or third parties), and the method(s) used to classify people into the different categories (e.g. self-report, census or administrative data, social media data, etc.)* *Please provide details about how you controlled for confounding variables in your analyses.*
Population characteristics	*Describe the covariate-relevant population characteristics of the human research participants (e.g. age, genotypic information, past and current diagnosis and treatment categories). If you filled out the behavioural & social sciences study design questions and have nothing to add here, write "See above."*
Recruitment	*Describe how participants were recruited. Outline any potential self-selection bias or other biases that may be present and how these are likely to impact results.*
Ethics oversight	*Identify the organization(s) that approved the study protocol.*

Note that full information on the approval of the study protocol must also be provided in the manuscript.

Field-specific reporting

Please select the one below that is the best fit for your research. If you are not sure, read the appropriate sections before making your selection.

☒ Life sciences ☐ Behavioural & social sciences ☐ Ecological, evolutionary & environmental sciences

For a reference copy of the document with all sections, see nature.com/documents/nr-reporting-summary-flat.pdf

Life sciences study design

All studies must disclose on these points even when the disclosure is negative.

Sample size	We did not calculate sample sizes beforehand. To ensure reliable estimation of PSF parameters across the field of view (FOV), we measured the full width at half maximum (FWHM) of seven nano-gold beads per FOV section, resulting in more than 300 beads in total in ASLM mode with and without the concave mirror. The beads were embedded in cleared, refractive-index-matched agarose within the chamber medium. For the mouse brain, cochlea, and zebrafish experiments, we did not use a statistical method to determine the number of samples. Instead, we imaged as many samples as were sufficient to demonstrate reproducibility and validate our imaging approach.
Data exclusions	No data was excluded.
Replication	Replication of the experiment on all imaged samples was successful.

Randomization	The PSF measurements were taken randomly across the large field of view.
Blinding	Not applicable. The manuscript describes a new imaging method.

Reporting for specific materials, systems and methods

We require information from authors about some types of materials, experimental systems and methods used in many studies. Here, indicate whether each material, system or method listed is relevant to your study. If you are not sure if a list item applies to your research, read the appropriate section before selecting a response.

Materials & experimental systems

n/a	Involved in the study
☐	☒ Antibodies
☒	☐ Eukaryotic cell lines
☒	☐ Palaeontology and archaeology
☐	☒ Animals and other organisms
☒	☐ Clinical data
☒	☐ Dual use research of concern
☒	☐ Plants

Methods

n/a	Involved in the study
☒	☐ ChIP-seq
☒	☐ Flow cytometry
☒	☐ MRI-based neuroimaging

Antibodies

Antibodies used

Mouse Cochlea:
Guinea pig polyclonal anti-parvalbumin antibody (Synaptic Systems, Cat.: 195 004; Lot # 3-38; Clone not specified) – dilution: 1:300
Camelid single domain anti-guinea pig antibody (NanoTag Biotechnologies, Cat.: N0602; Lot # 022205; Clone not specified) labelled with Atto565 – pre-conjugated with 195 004 (Synaptic Systems, see before) at a molar ratio of 1:3.

Multicolor imaging of mouse cochlea: guinea pig anti-parvalbumin (Synaptic Systems, Cat.: 195 004) and the camelid single domain anti-guinea pig antibody (NanoTag Biotechnologies, Cat.: N0602) were used as described before. Additionally, a monoclonal mouse anti-neurofilament 200 antibody (Sigma-Aldrich, Cat.: N5389; Lot # 099M4843V; Clone NE14) at a dilution of 1:400 and a polyclonal rabbit anti-vesicular glutamate transporter 3 antibody (Synaptic Systems, Cat.: 135 203; Lot # 1-47; Clone not specified) at a dilution of 1:300 were used..For the corresponding secondary staining staining an anti-mouse antibody labelled with Alexa 647 (Invitrogen, Cat.: A-21236; Lot # 751096; Clone not specified) and an anti-rabbit antibody labelled with Alexa 488 (Invitrogen; Cat.:, A-11008; # 659082; Clone not specified),were used, each at a dilution of 1:200..

Mouse brain:
Anti-α smooth muscle actin (αSMA) – Directly coupled to Cy3 (Millipore, C6198, 3.75 µg/ml, clone 1A4) - Used for detecting smooth muscle cells (validation: original publication: Skalli, O., et al. A monoclonal antibody against alpha-smooth muscle actin: a new probe for smooth muscle differentiation. J Cell Biol 103, 2787-2796 (1986).)
Anti-podocalyxin (R&D Systems, MAB1556, 0.5 µg/ml, clone 192703) - Used for detecting endothelial cells (validation: Monoclonal antibody used by numerous studies according to manufacturer, validated by the staining pattern)
Anti-CD31 (R&D Systems, AF3628, 0.133 µg/ml, lot not recorded) - Used for detecting endothelial cells (validation: Polyclonal antibody used by numerous studies according to manufacturer, validated by the staining pattern)
Anti-goat secondary antibody coupled to Alexa647 (Invitrogen, A21447, 2.5 µg/ml, lot: 2297623)
Anti-rat secondary antibody coupled to Alexa647 (Abcam, ab150155, 2.5 µg/ml, lot: 2465077)

Validation

The usage of all primary antibodies is described in the Methods section for both mouse cochlea and mouse brain preparations.
• Mouse cochlea:
Used for immunofluorescence staining in mouse cochlear tissue.
Duque Afsonso CJ: Development and Application of Tools for the Characterization of the Optogenetics Stimulation of the Cochlea. PhD Thesis. 2020; http://dx.doi.org/10.53846/goediss-8106

• Mouse brain:
• anti-αSMA: Used for immunofluorescence staining of smooth muscle actin in mouse brain vasculature; validated by Skalli, O., et al. A monoclonal antibody against alpha-smooth muscle actin: a new probe for smooth muscle differentiation. J Cell Biol 103, 2787–2796 (1986).
• anti-CD31: Used for immunofluorescence staining of endothelial cells in mouse brain tissue; validated by Western blotting according to manufacturer and by staining pattern; widely used in published studies.
• anti-podocalyxin: Used for immunofluorescence staining of vascular structures in mouse brain tissue; validated by immunocytochemistry according to manufacturer and by staining pattern; widely used in published studies.

Animals and other research organisms

Policy information about studies involving animals; ARRIVE guidelines recommended for reporting animal research, and Sex and Gender in Research

Laboratory animals	Mouse cochlea: Mus musculus, C57BL/6J. The mice were kept at a constant temperature of 22-24°C and at a relative humidity level of 45 to 65% on a 12-hour light/ dark cycle and were provided with enrichment, and access to food and water ad libitum. Mice for extraction of cochleae were bred at the local animal facility of the University Medical Center Göttingen. Here, we used C57BL/6J wild-type mice of both sexes of 1-2 months. Mouse Brain: C57BL/6N mice (bred in the animal facility of the University of Lübeck). The mice were kept at a constant temperature (22°C) and humidity (50%) on a 12-hour light/ dark cycle and were provided with standard laboratory chow and water ad libitum. Mice for brain extraction were bred at the local animal facility of the University of Lübeck. Male C57BL6/N mice at the age of 4-6 months were used. Zebrafish: transgenic line Tg(kdrl:GFP), 3 dpf
Wild animals	/
Reporting on sex	Mouse Cochlea: Animals of both sexes were used. Mouse Brain: both sexes weres used for establishing stainings and clearing, no difference was observed, images in the manuscript originate from male mice Zebrafish: The sex cannot be determined at this early stage of development.
Field-collected samples	/
Ethics oversight	In Germany organ extraction is operated under §4 of the animal wellfare act and not requiring specific permission of the responsbile authorities. Following internal regulations, approval for extraction of cochleae was obtained from the animal welfare office of the University Medical Center (UMG) Göttingen. At University Medical Center Göttingen animals for this study were strictly sacrificed for organ collection only. Thus, a license by the authorities was not required. It was performed according to the regulations of the internal animal welfare office. Experimental procedures were approved by the local animal ethics committee (Ministerium für Landwirtschaft, Umwelt und ländliche Räume, Kiel, Germany). Adult zebrafish (Danio rerio), embryos and larvae were maintained following established protocols in compliance with EU directive 2010/63/EU and the German Animal Welfare Act and approved by the authorities of Lower Saxony (Niedersächsisches Landesamt für Verbraucherschutz und Lebensmittelsicherheit, Oldenburg, Germany).

Note that full information on the approval of the study protocol must also be provided in the manuscript.

Plants

Seed stocks	*Report on the source of all seed stocks or other plant material used. If applicable, state the seed stock centre and catalogue number. If plant specimens were collected from the field, describe the collection location, date and sampling procedures.*
Novel plant genotypes	*Describe the methods by which all novel plant genotypes were produced. This includes those generated by transgenic approaches, gene editing, chemical/radiation-based mutagenesis and hybridization. For transgenic lines, describe the transformation method, the number of independent lines analyzed and the generation upon which experiments were performed. For gene-edited lines, describe the editor used, the endogenous sequence targeted for editing, the targeting guide RNA sequence (if applicable) and how the editor was applied.*
Authentication	*Describe any authentication procedures for each seed stock used or novel genotype generated. Describe any experiments used to assess the effect of a mutation and, where applicable, how potential secondary effects (e.g. second site T-DNA insertions, mosiacism, off-target gene editing) were examined.*

nature biotechnology

Supplementary information

https://doi.org/10.1038/s41587-025-02882-8

Isotropic, aberration-corrected light sheet microscopy for rapid high-resolution imaging of cleared tissue

In the format provided by the authors and unedited

Table of contents

Supplementary Note 1. Resolution and depth of field of Multi-immersion Objective
Supplementary Note 2. Vasculature segmentation and tracing
Supplementary Note 3. Practical considerations for mitigating aberrations
Supplementary Note 4. Voice coil calibration procedure
Supplementary Fig. 1. Resolution calculation for multi-immersion objective lens.
Supplementary Fig. 2. Schematic of the cleared tissue light sheet microscope.
Supplementary Fig. 3. 3D rendering of the cleared tissue optical setup.
Supplementary Fig. 4. Mechanical details of the assembly of the voice coil, position sensing device (PSD), and chamber.
Supplementary Fig. 5. Frequency response of the voice coil measured with the position sensing device.
Supplementary Fig. 6. Mouse brain preparation for imaging.
Supplementary Fig. 7. Segmentation and tracing of two selected penetrating arterioles.
Supplementary Fig. 8. Electronics components and their electrical waveforms.
Supplementary Table 1. Comparison between the tested sCMOS cameras.
Supplementary Table 2. Microscope parts list

Supplementary Note 1. Resolution and depth of field of the multi-immersion objective lens

The theoretical resolution and imaging depth of field (DOF) are presented in this section for the ASI objective lens with NA 0.4. The calculated parameters are sorted by varying the tube lens and magnification to make it easier to follow the resolution and DOF behavior (**Supplementary Fig. 1**). The tube lenses are chosen from the 160–300 mm focal length range, which provide magnifications of 13–25×. For tube lenses with focal lengths less than 200 mm, the lateral resolution and magnification increase as the focal length of the tube lens approaches 200 mm. Following that, the resolution remains constant as it is limited by the camera's pixel pitch of 6.5μm. The highest resolution achievable with the objective lens is then given by the objective lens' NA. For instance, for a refractive index of 1.56 and a tube lens of f=200 mm or longer, the highest theoretical achievable resolution for the ASI lens with an NA of 0.4 is 740nm. The depth of field (DOF) of the objective lens decreases as the focal length of the tube lenses is increased. This is because the DOF and magnification have an inverse relationship. Thus, increasing the magnification decreases the DOF. As a result, the optimal tube lenses for the ASI lenses have a focal length of 200 mm to achieve the highest resolution possible.

Supplementary Note 2. Vasculature segmentation and tracing

Mouse brain vasculature segmentation was performed using a local contrast method in Imaris 9.6.1 to enhance vessel visibility against the background. The analysis was conducted at the original resolution without any downsampling, and no smoothing was applied to preserve the fine structural details of the vasculature. Each segmentation block consisted of a 3D cropped volume centered on an individual penetrating artery, with an average volume of 500 μm × 500 μm × 500 μm. The segmentation was initially executed using the Surface module in Imaris to generate a volumetric representation of the main artery. Smaller segmented particles that did not belong to the arterial tree were excluded—first through thresholding based on segmented volume, and then through manual inspection to eliminate any remaining irrelevant structures. The resulting clean surface segmentation of the arterial tree was then used as a baseline for the Filament Tracer module in Imaris, which was utilized to automatically trace and reconstruct the artery's sub-branches and the surrounding vascular network.

Supplementary note 3. Practical considerations for mitigating aberrations

This study focuses on spherical aberrations and field curvature, as they are the primary limitations in high-resolution imaging across large fields. However, asymmetric aberrations—such as astigmatism and coma—can also occur, typically due to potential optical or mechanical misalignments. In our system, these aberrations were not observed after careful alignment. Since coma aberrations may be caused by off-axis beam propagation, in our setup, the most critical point where this can occur is at the entrance to the meniscus lens. If the beam exiting the illumination objective lens is not well aligned with the optical axis of the meniscus lens, coma aberration can be introduced to the light sheet. Additionally, misalignment between the detection objective's focal plane and the meniscus lens can cause the light sheet to enter off-axis, which may also increase the potential of coma aberration. These issues can be avoided by precisely aligning the optical components and carefully designing the chamber to ensure the meniscus lens optical axis aligns with the detection objective lens's focal plane.

Astigmatism is another expected aberration in conventional light sheet imaging, especially when using glass capillaries to mount samples. However, in our system, this aberration was negligible due to the overall imaging principle, which ensures that the refractive index (RI) of the sample matches that of the chamber medium. For rigid samples, the sample can often be directly immersed in the chamber medium, allowing for complete RI matching between the sample and the medium, which reduces the potential for astigmatism aberration. For fragile samples that require more secure mounting in glass capillaries, minimizing astigmatism relies on matching the RI of the cleared sample and the chamber medium to that of the capillary glass.

Supplementary note 4. Voice coil calibration procedure

To calibrate the voice coil movement, we performed the following three steps:

Step 1 – Empirical measurement of light sheet shift. We first empirically measured the shift of the light sheet for each 1 mV step and observed that each 1 mV corresponds to a 4 μm shift in the chamber. We also determined that the effective light sheet length (twice the Rayleigh range) is 8 μm. To maintain optimal optical thickness, the voice coil movement must remain within 4 μm (i.e., the Rayleigh range). This sets our predefined metric: the maximum residual error in the sweep should not exceed 4 μm, corresponding to 1 mV.

Step 2 – Iterative waveform correction. We recorded the response of the voice coil to a linear ramp function using the PSD. The recorded data was smoothed to reduce noise. We identified the minimum and maximum of the smoothed signal and aligned them with the endpoints of the ramp. The residual waveform was calculated by subtracting this signal from the ideal ramp. We quantified both the peak residual and its standard deviation (σ). A sweep was considered acceptable when the peak residual was below 1 mV and σ below 0.24 mV. If these criteria were not met, the inverted residual was added to the input to generate a corrected waveform. This iterative process—measure, correct, reapply—was repeated until both thresholds were met. This ensures the beam remains synchronized with the rolling shutter and within the optical limits imposed by the Rayleigh range.

Step 3 – User-guided validation of beam quality. The refined waveform was then used to drive the voice coil, and the resulting swept beam was evaluated manually. As a secondary quality metric, the beam should maintain consistent thickness across the field of view. Users inspected the beam profile at multiple positions by extracting and comparing line profiles. If any fluctuations in beam size were observed, this indicated residual errors persisted. In such cases, Step 2 was repeated for further fine-tuning.

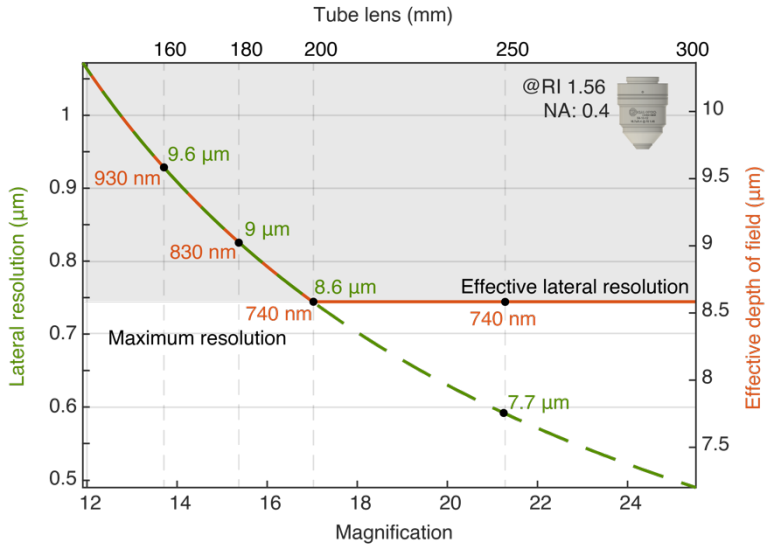

Supplementary Fig. 1. Resolution considerations for multi-immersion objective lens. Lateral resolution and effective depth of field for the ASI lens with NA 0.4 are calculated in relation to the magnification and focal length of the tube lens. The solid orange and dashed green lines represent the lateral resolution and DOF, respectively. The grey area indicates the achievable resolution with a camera pixel pitch of 6.5μm.

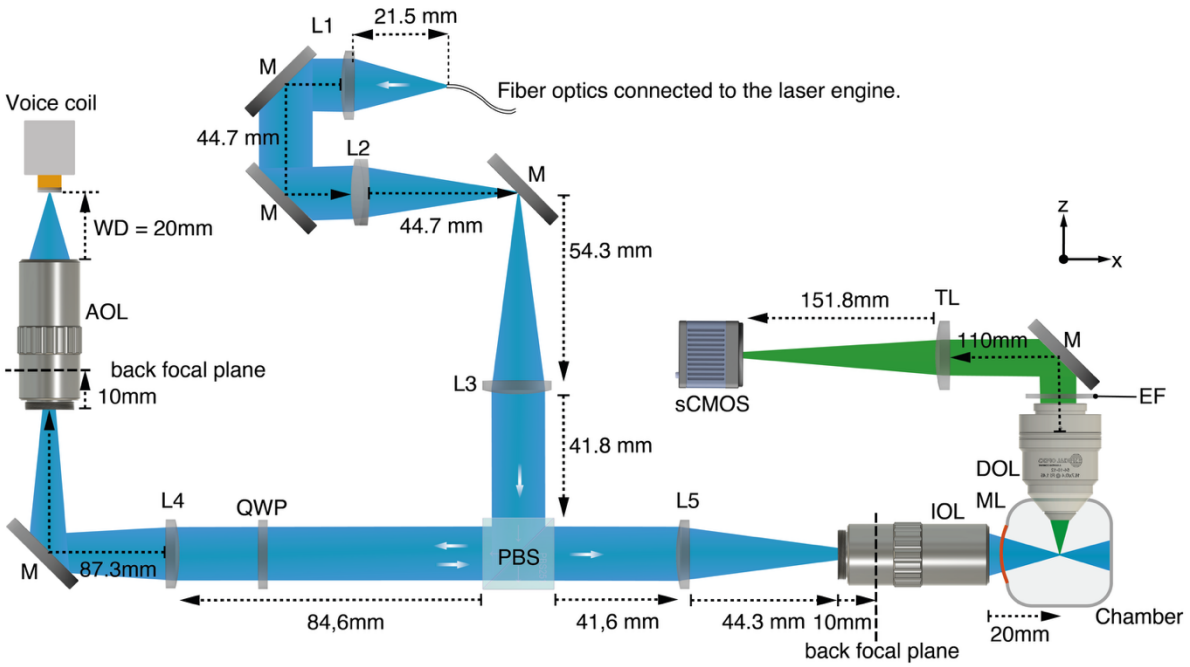

L1: Collimator lens, F = 25 mm, Fb = 21.5 mm (Fb indicates back focal plane)
M: Mirror
L2: Cylindrical lens, F = 50 mm, Fb = 44.7 mm
L3: Expander lens, F = 60 mm, Fb = 54.3 mm
PBS: Polarizing beamsplitter
QWP: Achromatic quarter-waveplate
L4: ASLM's tube lens, F = 100 mm, Fb = 97.3 mm
AOL: ASLM's objective lens, WD = 20 mm, Fb = 10 mm (inside the objective from rear thread)
ASLM's mirror: Concave mirror, F = 9.5 mm
L5: Illumination tube lens, F = 60 mm, Fb = 54.3 mm
IOL: Illumination objective lens, WD = 20 mm, Fb = 10 mm (inside the objective from rear thread)
ML: Positive meniscus lens, F = 100 mm
DOL: Multi-immersion detection objective lens, WD = 12 mm
EF: Emission filter
TL: Detection tube lens, F = 200 mm, WD = 151.8 mm, Pupil distance = 110 mm (working range: 70–170 mm)
sCMOS: Camera with light sheet mode

Supplementary Fig. 2. Schematic of the cleared tissue light sheet microscope, illustrating the actual physical distances between all optical components. Dashed arrowheads indicate the precise distance between the faces of two adjacent optical elements. At the bottom of the schematic, abbreviations for each optical element are listed alongside their optical parameters. "F" represents the focal length of the lenses, and "Fb" indicates the back focal plane. All optical components are chosen from achromatically designed optical elements to cover the full visible spectrum.

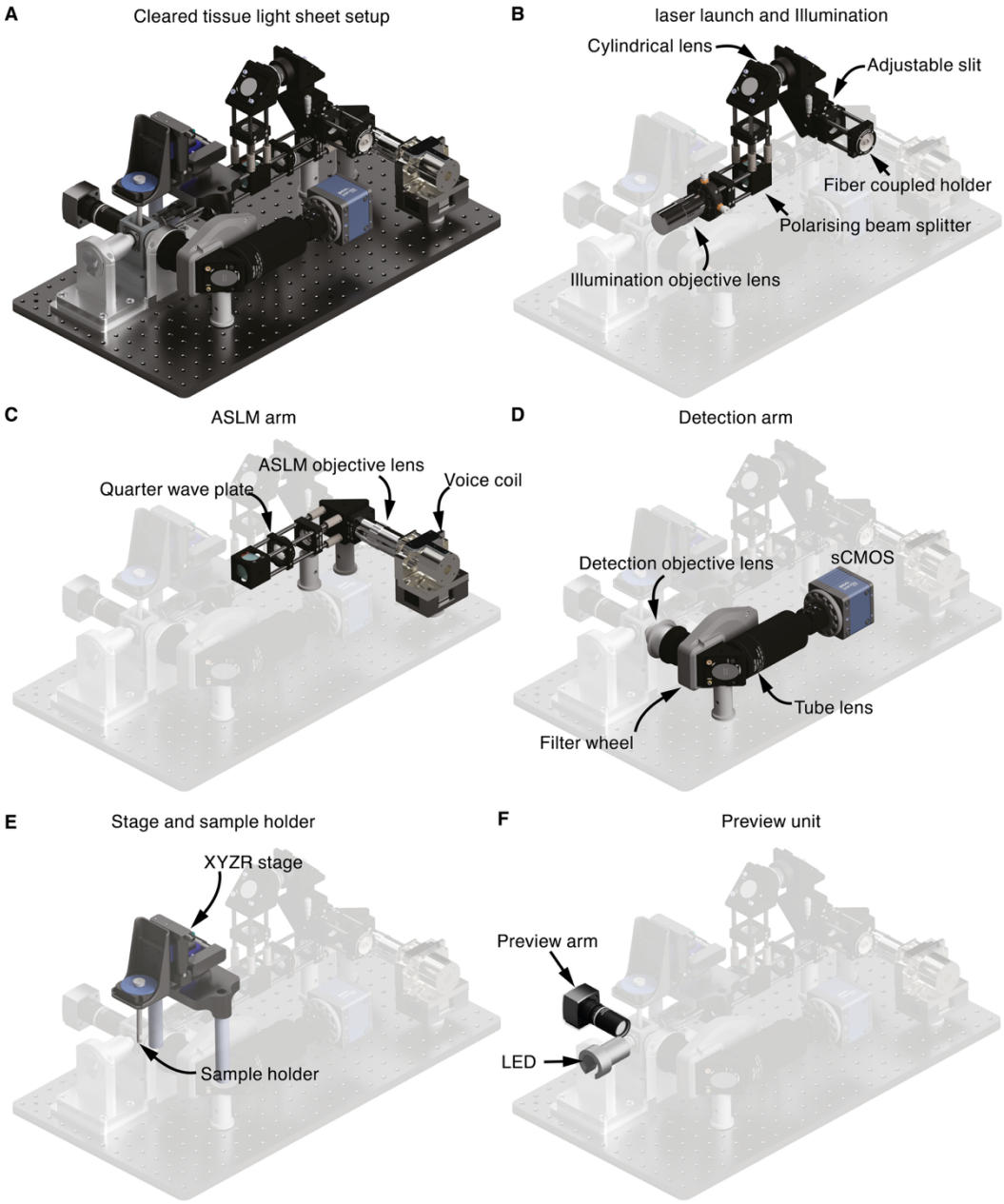

Supplementary Fig. 3. 3D rendering of the cleared tissue optical setup. A, 3D rendering of the entire setup. **B**, laser launch and illumination arm. **C**, ASLM arm. **D**, detection arm. **E**, sample stage and holder. **F**, preview unit. The base plate's size is 30x60 cm^2.

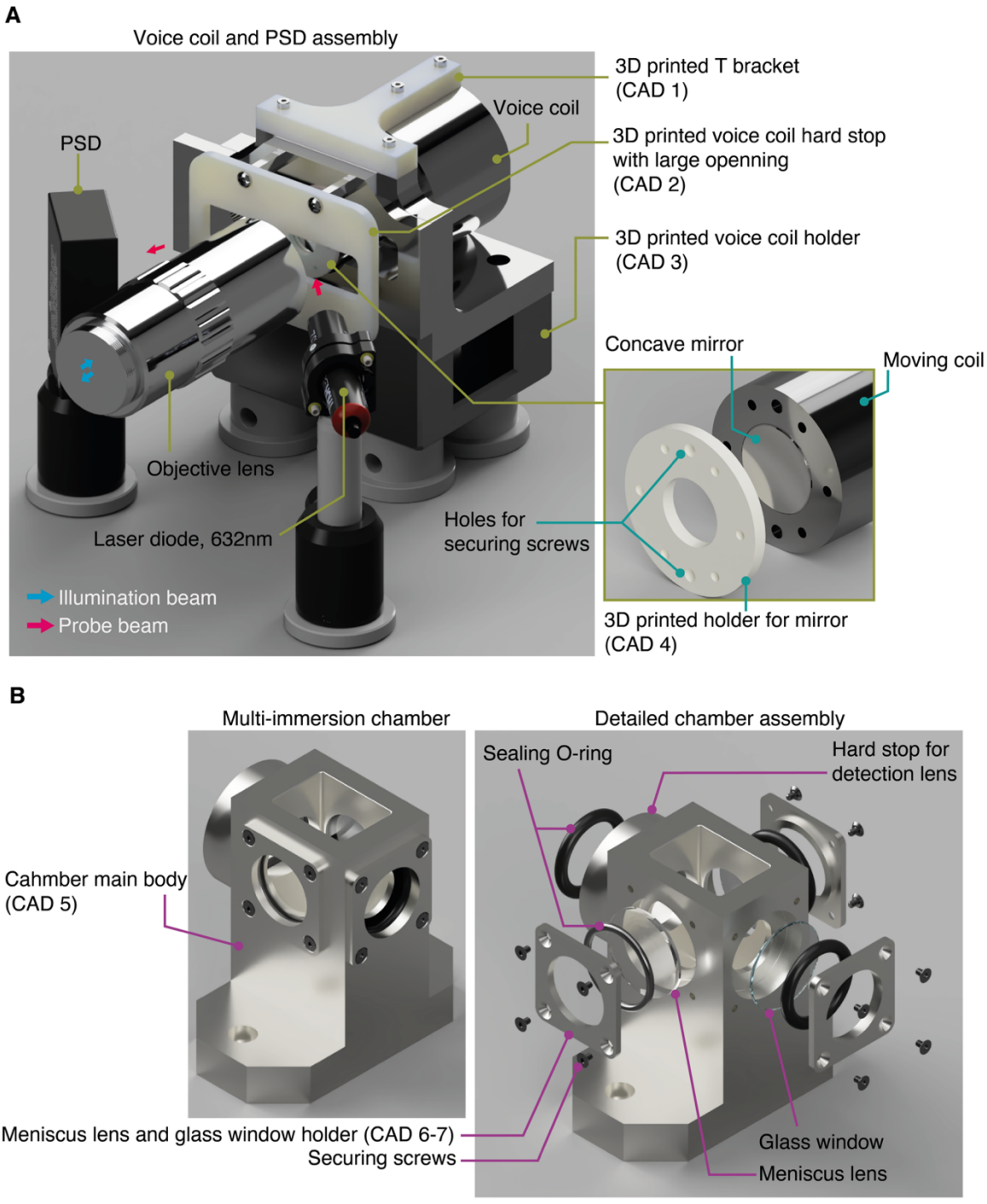

Supplementary Fig. 4. Mechanical details of the assembly of the voice coil, position sensing device (PSD), and chamber. A, assembly of the voice coil, including all 3D-printed parts and the holder. A T-bracket is printed and attached to the voice coil to dampen unnecessary vibrations. The hard stop is also 3D-printed using a rigid material, with a widened horizontal opening that allows the probe laser line to enter and reflect seamlessly toward the PSD, as indicated by the red arrowhead. The entire voice coil is mounted and held by a 3D-printed holder, which is supported by stainless steel legs. In the right image, the core of the moving coil is magnified to show where and how the concave mirror is secured using a 3D-printed ring holder. **B**, Left: overview of the CAD model of the multi-immersion chamber. Right: exploded view of all detailed components of the chamber, including holders, meniscus lens, glass windows, and O-rings, as well as the placement of the hard stop for detection. The hard stop is positioned to keep the front of the multi-immersion lens precisely 12 mm (the working distance for all refractive indices) from the illumination optical axis, aligned with the center of the meniscus lens.

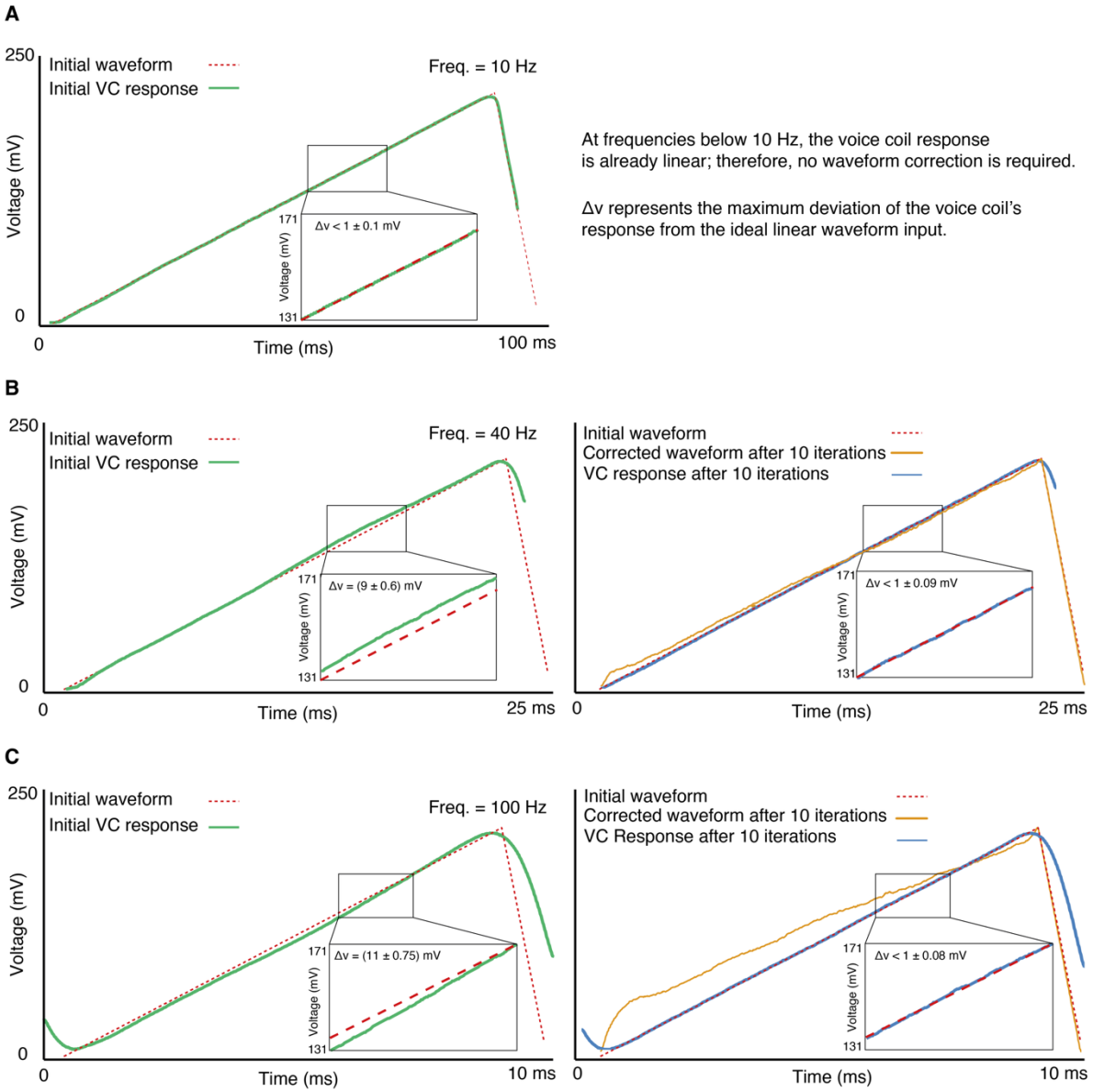

Supplementary Fig. 5. Frequency response of the voice coil (VC) measured with the position sensing device (PSD). A, Input ramp waveform at 10 Hz (red dashed line) and the corresponding VC response recorded by the PSD (green solid line). Inset: an enlarged view of the recorded waveform and the calculated maximum deviation. B, Left: 40 Hz ramp waveform and VC response (green solid line). Inset: an enlarged view of the recorded waveform and the calculated maximum deviation. Right: VC response after 10 iterations (green-blue line) and the corrected waveform (orange solid line). Inset: an enlarged view of the recorded waveform and the calculated maximum deviation. **C**, Left: 100 Hz ramp waveform and VC response (green solid line). Inset: an enlarged view of the recorded waveform and the calculated maximum deviation. Right: VC response after 10 iterations (green-blue line) and the corrected waveform (orange solid line). Inset: an enlarged view of the recorded waveform and the calculated maximum deviation.

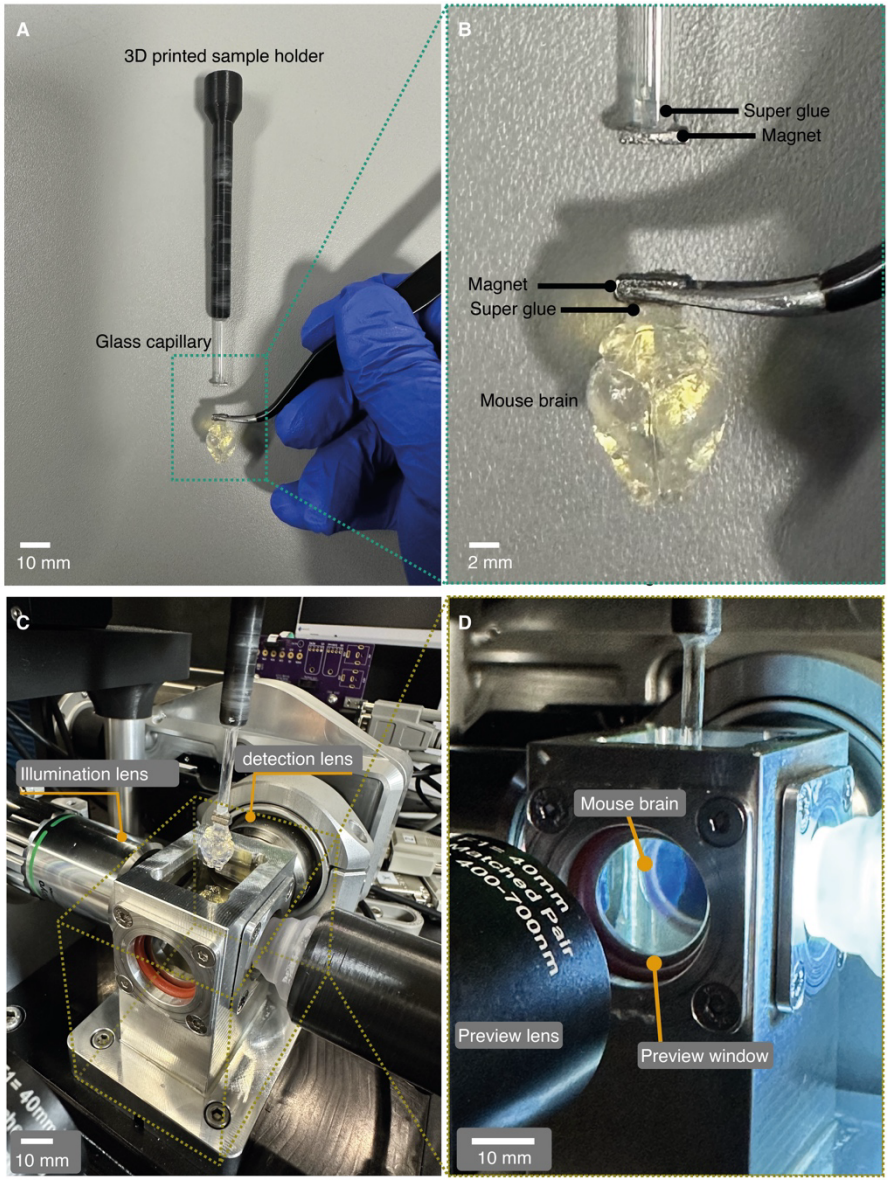

Supplementary Fig. 6. Mouse brain preparation for imaging. A, A cleared mouse brain is glued to a magnet using super glue and a 3D-printed sample holder secures a glass capillary with another magnet at its tip. **B**, Enlarged view of the mouse brain shown in A. **C**, An illumination objective lens, a detection objective lens, and an LED with a 3D-printed holder surround a chamber filled with ECi. **D**, The cleared mouse brain inside the chamber is visible through a preview window facing the preview lens.

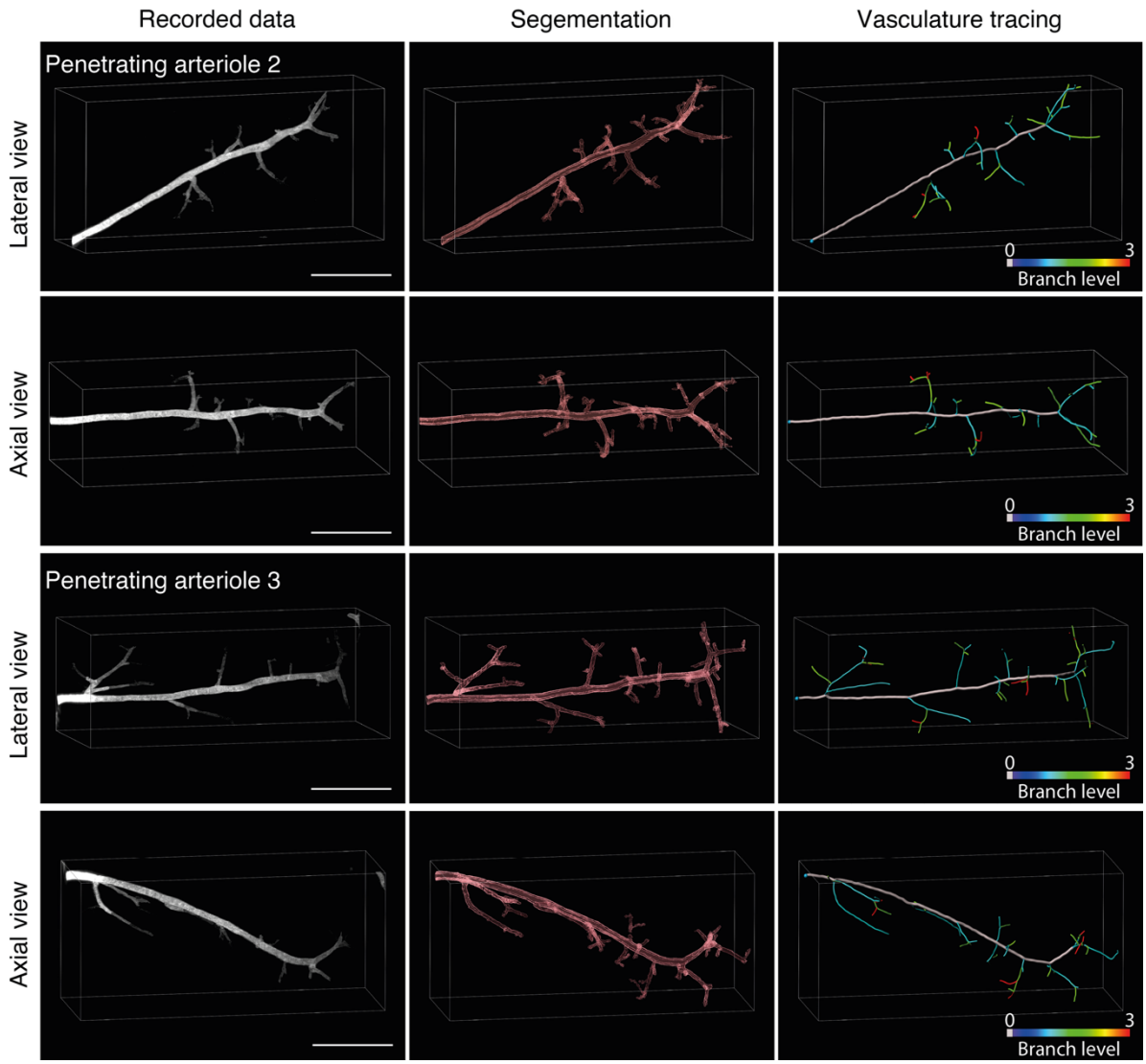

Supplementary Fig. 7. Segmentation and tracing of two selected penetrating arterioles from Figure 6E. The first column: the recorded data of two penetrating arterioles in both lateral and axial views. The middle column: segmentation of the corresponding vessels. The images are an example from one of two imaged samples. The third column: vasculature tracing. The color-coded tracing shows the sub-branch levels. Scale bars: 200 µm

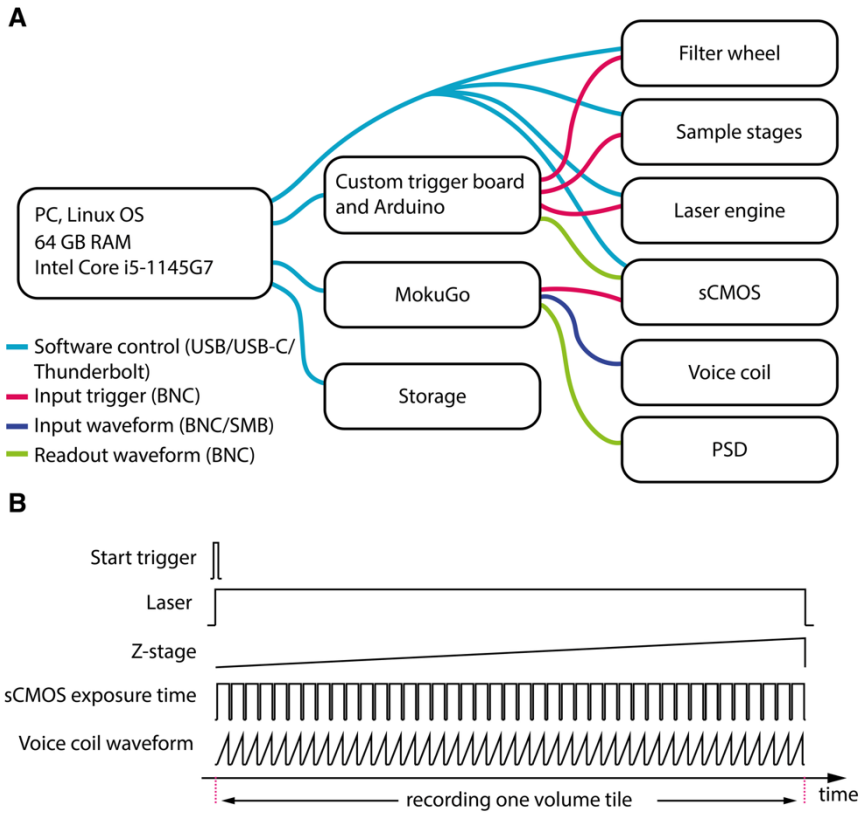

Supplementary Fig. 8. **Electronic components and their electrical waveforms. A**, The microscope is run by a small Linux computer. All components are either directly connected to the computer via USB or connected to trigger boards, such as custom boards, Arduino, and MokuGo. The recorded data is streamed to a solid-state drive (SSD). **B**, The microscope's components are started by a user command, and a trigger board sends signals to the other components, such as the laser, z-stage, sCMOS, and voice coil.

Supplementary table 1. Comparison between the tested sCMOS cameras.

sCMOS parameters in light sheet mode	pco.panda 4.2	Hamamatsu Orca-Fusion	pco.edge 10bi
Maximum frame rate (Hz)	40	100	120
Achieved frame rate in ASLM mode (Hz)	32	84	100
Exposure line (µs)	12.136	4.868	6.84
Chip size (pixel)	2048x2048	2304x2304	4416x2368
Used chip (pixel)	2048x2048	2048x2048	2368x2368
Effective FOV (µm x µm)	780x780 (TL: 200mm)	780x780 (TL: 200mm)	625x625 (TL: 200mm) 750X750 (TL:160mm)
Volume imaging speed of 1mm^3 (4000 images)	2.2 min	45 sec	32 sec
Camera connection	USB-C	Frame grabber	Frame grabber

Supplementary table 2. Microscope parts list

Item	Part name	Quantity	Supplier	Cost $
Positive Meniscus Lens	LE1234	1	Thorlabs	25
Concave mirror	CM127-010-P01	1	Thorlabs	46
Achromatin lens f: 25 mm	AC127-025-A-ML	1	Thorlabs	100
Achromatin lens f: 60 mm	AC254-060-A	2	Thorlabs	190
Achromatin lens f: 100 mm	AC254-100-A	1	Thorlabs	93
Glass window	WG11010	2	Thorlabs	187
Adjustable slit	VA100CP/M	1	Thorlabs	328
Polarizing Beamsplitting	CCM1-PBS251/M	1	Thorlabs	376
Emission filter	Filters	6	Thorlabs	2281
Cylindrical lens	ACY254-050-A	1	Thorlabs	478
Tube lens	TTL200-A	1	Thorlabs	573
Mirror	BB1-E02-10	1	Thorlabs	782
Halfwave plate	10RP52-1B	1	Newport	1222
Quarterwave plate	10RP54-3B	1	Newport	1222
Illumination Objective lens	MY20X-804 20X Plan Apochromat	1	Mitutoyo / Thorlabs	2613
ASLM Objective lens	MY20X-804 20X Plan Apochromat	1	Mitutoyo / Thorlabs	2613
Detection objective lens	Multi-immersion Objective lens, 54-10-12	1	Special optics / ASI	17000
Function generator	MokuGo	1	Liquid instrument	600
Voice coil	BLINK high-speed focuser	1	Thorlabs	5226
Sample stage	3X M1-112 DC motor, 1X U-628.03	1	Physik instrumente	18214
Camera	PCO Panda 4.2m	1	Excelitas	8000
Mechanical hardware and 3D prints	Mechanical hardware and 3D prints	1	-	5000
Laser engine	Laser Engine (CLE 25mW) / OBIS CellX 100 mW	1	Toptica / Coherent	27700
			Total cost	**94844**